

# Hydrogenation of Adsorbed Ethylene on ZnO(0001) Surface: Probed by Coherent Anti-Stokes Raman Scattering Spectroscopy Using Guided Waves

W. M. K. P. Wijekoon<sup>\*,†,‡</sup> and W. M. Hetherington, III

Contribution from the Department of Physics, Oregon State University, Corvallis, Oregon 97331

Received September 29, 1992

**Abstract:** Hydrogenation of ethylene adsorbed on ZnO(0001) surface was investigated with coherent anti-Stokes Raman spectroscopy (CARS) using a planar optical waveguide geometry. The CARS signal from the adsorbate layer was enhanced by choosing a combination of guided waves to minimize the contributions from the ZnO film. Spectra in the region of the  $\nu_1$  stretch provided evidence of the presence of several different types of adsorbed ethylene on the ZnO surface. These species exhibited  $\nu_1$  frequencies of surface retained ethylene around 1613, 1602, 1584, 1573, and 1553  $\text{cm}^{-1}$ , and sites are expected to be  $\text{Zn}^{2+}$  ions. The adspecies with the  $\nu_1$  frequency centered around 1602  $\text{cm}^{-1}$  undergo complete hydrogenation. The other species do not seem to be fully hydrogenated.

## Introduction

Metals and metal oxides are well-known catalysts for hydrogenation and isomerization of alkenes.<sup>1-3</sup> Over metals the hydrogenation reaction is very complex, with self-hydrogenation and dimerization of alkenes taking place, resulting in a variety of carbonaceous species. However, over oxide surfaces, in particular over ZnO, the hydrogenation of ethylene occurs in much simpler fashion without self-hydrogenation and dimerization.<sup>4-6</sup> The simplicity of the reaction is evident in the observations that the addition of deuterium to ethylene only yields  $\text{C}_2\text{H}_x\text{D}_2$ , whereas over metals a distribution of products ( $\text{C}_2\text{H}_{6-x}\text{D}_x$ , where  $0 \leq x \leq 6$ ) is obtained. The implications are that the addition of the first hydrogen is irreversible and that the confined structure of the resulting intermediate limits further reactions to the single path of addition of a second hydrogen. This relatively simple nature of the heterogeneous catalysis process makes ZnO a better candidate for investigations of chemistry behind ethylene hydrogenation.

The catalytic activity of ZnO in ethylene hydrogenation was recognized as early as 1940.<sup>7</sup> Since then a number of investigations have been made on the catalytic and related aspects of zinc oxide.<sup>4-6,8-12</sup> In a schematic series of chemical and spectroscopic studies, Kokes and his colleagues made progress in elucidating the mechanism of ethylene hydrogenation on a highly irregular surface of ZnO powder.<sup>4-6</sup> The general conclusion was that a limited number of surface sites ( $\approx 5\%$  of Zn-O pairs) which are capable of dissociative adsorption of hydrogen support the hydrogenation reaction, even in the presence of surface hydroxyls. It was speculated that the intermediate in the reaction is a Zn- $\text{C}_2\text{H}_5$  complex. The observation of a single broad IR peak around 1600  $\text{cm}^{-1}$ , on a rising background due to interference from ZnO, was interpreted as evidence of a single initial chemisorbed ethylene

species for which the frequency of the  $\nu_1$  ( $\nu_{\text{C}=\text{C}}$ ) has been reduced by 21  $\text{cm}^{-1}$  by the formation of  $\pi$ -complex with the surface. The heat of adsorption was measured to be 14  $\text{kcal mol}^{-1}$ .

However, latter studies reported the presence of at least two different types of surface-retained ethylene on the ZnO surface.<sup>10</sup> The adspecies which is chemisorbed almost exclusively as a weakly bound form with a heat of absorption of 4 to 6  $\text{kcal mol}^{-1}$  is hydrogenated. The other form which is adsorbed in much smaller amounts is not hydrogenated. These authors have degassed excess ethylene before the measurements, and therefore, their results do not necessarily correspond to that of Dent and Kokes. A large portion of weakly bound ethylene could have been removed during the evacuation. The other investigators measured four distinct heats of adsorption of 0, 4, 13, and  $>13$   $\text{kcal mol}^{-1}$  and concluded that three chemisorbed species are present along with physisorbed ethylene.<sup>12</sup>

In our earlier paper we presented spectroscopic evidence for the presence of at least four different types of adsorbed ethylene on a partially hydroxylated ZnO(0001) surface.<sup>13</sup> We were able to detect different types of surface-bound ethylene on a well-defined (0001) surface of ZnO by performing CARS spectroscopy in the planar waveguide geometry. Previous IR studies had neither spectral resolution nor the homogeneity of the surface structure necessary for the observation of all these species. Furthermore, we found that some of the surface-retained ethylene is strongly bonded to the surface and therefore cannot be recovered with a brief evacuation of the sample chamber. A complete removal of adsorbed ethylene required heating of the ZnO surface. Also, it was evident that the population of some of the chemisorption sites was controlled by the diffusion of adspecies among the adsorption sites. At relatively higher surface pressures observation of all the species was difficult due to the presence of a thin hydroxyl coating on the surface. Under the experimental conditions used in the present work, surface hydroxyl density is largely reduced, and all the previously observed surface species could be seen very easily. The purpose of this work is to apply the waveguide surface CARS technique to study the catalytic activity of different types of surface-retained ethylene on ZnO.

## Theoretical Background

The concept of waveguide surface CARS (WSCARS) involves three wave mixing with the evanescent fields above an optical

\* Department of Chemistry, University of Arizona, Tucson, AZ 85721.

† Present address: Photonics Research Laboratory, Department of Chemistry, The State University of New York at Buffalo, Buffalo, New York 14214.

(1) Taylor, T. I. *Catalysis*; Emmet, P.H., Ed.; Reinhold Publishing Co.: New York, 1957; Vol. V.

(2) Harrison, D. L.; Nicholls, D.; Steine, H. *J. Catal.* **1967**, *7*, 359.

(3) Eischens, R. P.; Pliskin, W. a. *Adv. Catal.* **1978**, *10*, 1.

(4) Dent, A. L.; Kokes, R. J. *J. Phys. Chem.* **1969**, *73*, 3772.

(5) Dent, A. L.; Kokes, R. J. *J. Phys. Chem.* **1969**, *73*, 3781.

(6) Dent, A. L.; Kokes, R. J. *J. Phys. Chem.* **1970**, *74*, 3653.

(7) Woodman, J. F.; Taylor, H. S. *J. Am. Chem. Soc.* **1940**, *62*, 1393.

(8) Aigueperse, J.; Teichner, S. J. *J. Catal.* **1963**, *2*, 395.

(9) Bozon-Verdravaz, F.; Teichner, S. J. *J. Catal.* **1968**, *11*, 7.

(10) Baranski, A.; Cvetanovic, R. J. *J. Phys. Chem.* **1971**, *75*, 208.

(11) Ismail, T. Ali.; Gay, D. J. *Catal.* **1980**, *62*, 341.

(12) Yuseke Yasuda *J. Phys. Chem.* **1976**, *80*, 1870.

(13) Wijekoon, W. M. K. P.; Ho, Z. Z.; Hetherington, W. M. *J. Chem. Phys.* **1987**, *86*, 4384.

waveguide.<sup>14,15</sup> The waveguide structure consists of a substrate (silica), film (ZnO), and superstrate (monolayer or air). When the refractive index of the film is greater than that of the substrate and the superstrate, an optical field can be constrained by total internal reflection and will propagate through the film as a guided wave. The two input fields at  $\omega_1$  and  $\omega_2$  are coupled into the film through an optically contacted prism, and the field at  $\omega_3 (= 2\omega_1 - \omega_2)$ , which is generated as a guided wave, is coupled out of the film via another prism.

The planar optical waveguide geometry intensifies the optical fields by virtue of the small film thickness, a fact which permits CARS to occur with relatively little laser power. Coherent Raman scattering benefits from the waveguide geometry to a much greater extent than spontaneous Raman scattering.<sup>16</sup> Since the CARS intensity is quadratic in the interaction distance of the two input fields, the long interaction length ( $\sim 1$  cm) within the waveguide leads to very high conversion efficiencies. The surface sensitivity of WSCARS can be greatly enhanced by establishing an interference condition in the film.<sup>13</sup>

With use of the coupled mode theory, the power in the WSCARS beam can be written as follows:<sup>17</sup>

$$P_{\text{CARS}} \propto C \left( \frac{L}{W} \right)^2 |F|^2 P_1^2 P_2 \quad (1)$$

where  $L$  is the interaction length inside the film,  $P_1$  and  $P_2$  are the powers at input frequencies  $\omega_1$  and  $\omega_2$ ,  $W$  is the width of the guided beam, and

$$F = \int_{-\infty}^{\infty} \chi^3(z) f_1^2(z) f_2(z) f_3(z) dz \quad (2)$$

where  $f_i$  is the distribution function for the field at  $\omega_i$ . The third-order susceptibility,  $\chi^{(3)}$ , contains vibrationally resonant and nonresonant (background) terms. When TE modes are used for the fields at  $\omega_i$ , only  $\chi_{xxxx}^{(3)}$  is measured. Other components of  $\chi^{(3)}$  can be measured by using combinations of different TE and TM modes for the input and signal fields. Although the CARS signal from a monolayer is large and detectable, the signal from the nonresonant susceptibility of the film is much larger. The background contribution to the CARS signal can be suppressed by the proper choice of guided modes for the input and output laser fields.

The third-order susceptibility,  $\chi^{(3)}$ , in eq 2 can be resolved into different components as follows: monolayer,  $\chi_m^{(3)} = \chi_{mr}^{(3)} + \chi_{mb}^{(3)}$  (resonant and nonresonant contributions), film,  $\chi_f^{(3)}$ , and substrate,  $\chi_s^{(3)}$ . Then the tensor,  $F$ , becomes

$$F = \int_{-\infty}^{\infty} [\chi_m^{(3)}(z) + \chi_s^{(3)}(z) + \chi_f^{(3)}(z)] f_1^2(z) f_2(z) f_3(z) dz \quad (3)$$

By choosing TE modes for the three fields such that the product  $f_1^2 f_2 f_3$  is antisymmetric across the film,

$$\int_{\text{film}} \chi_f^{(3)}(z) f_1^2(z) f_2(z) f_3(z) dz \approx 0 \quad (4)$$

and the CARS signal arises mainly from the monolayer and the substrate only. The total CARS signal is

$$P_3 \propto |A|^2 + AB^* + A^*B + |B|^2 \quad (5)$$

where

$$A = \int_{\text{monolayer}} \chi_m^{(3)}(z) f_1^2(z) f_2(z) f_3(z) dz \quad (6)$$

$$B = \int_{\text{substrate+film}} [\chi_s^{(3)}(z) + \chi_f^{(3)}(z)] f_1^2(z) f_2(z) f_3(z) dz \quad (7)$$

When the CARS signal from the monolayer ( $A$ ) is small, the surface signal may appear through the cross term in eq 5. By optimizing the thickness of the waveguide, the surface signal can be three orders of magnitude larger than the background signal.<sup>13</sup>

### Experimental Aspects

A detailed description of the WSCARS spectrometer and the experimental geometry have been given previously,<sup>19-21</sup> and only the details pertinent to this study will be presented here. The ZnO film (thickness =  $0.60 \pm 0.03 \mu\text{m}$ ) was deposited onto a silica substrate in an RF magnetron sputtering plant.<sup>22</sup> The optical loss in the ZnO waveguide was determined to be  $\sim 5$  db  $\text{cm}^{-1}$  for modes  $\text{TE}_1$  and  $\text{TE}_2$  at 602 nm. Two  $\text{SrTiO}_3$  prisms were employed to couple the laser beam into and out of the waveguide. Optical coupling was achieved by varying the contact pressure between the prism and the ZnO film. The two input beams entered the prism with a small angular separation in both YZ and XY planes and were focused onto the optical contact area of the prism. The approximate coupling angles used for the  $\text{TE}_1$  ( $\omega_1$ ),  $\text{TE}_1$  ( $\omega_2$ ), and  $\text{TE}_2$  ( $\omega_3$ ) modes were  $16^\circ$ ,  $14^\circ$ , and  $3^\circ$ , respectively. The coupling angles did not need to be changed during a scan over as much as  $100 \text{ cm}^{-1}$ . The above-mentioned 112-mode combination was chosen due to the geometrical constraint of the vacuum chamber system and the anticipated favorable ratio of the monolayer-to-background signals. The width of each guided beam was  $\sim 200 \mu\text{m}$  and the interaction distance was  $\approx 2$  mm. Thus surface area probed by the CARS was only  $0.4 \text{ mm}^2$ , which meant a maximum of only  $4 \times 10^{11}$  adspecies could be sampled.

It should be noticed that the CARS signals reported in this work are considerably lower than those in a phased matched situation since the WSCARS process cannot be phase matched for the 112-mode combination with any choice of angle in the XY plane. However, presence of a phase mismatch does not significantly interfere with analysis of a spectrum.<sup>13</sup>

The laser system used for this investigation consisted of two dye lasers which were synchronously pumped by the frequency-doubled output of a mode-locked  $\text{Nd}^{+3}$ :YAG laser which was Q-switched at 500 Hz. The individual pulses within each pulse train were approximately 50 ps in duration and had a spectral line width of  $1.3 \text{ cm}^{-1}$ . The approximate laser wavelengths used were 557 nm (fixed) for  $\omega_1$  and 612 nm (tunable) for  $\omega_2$ , and the entire dye laser pulse trains were used. During a CARS scan, the wavelength of  $\omega_2$  laser was continuously monitored with a 1-m monochromator. The surface CARS signal generated in the desired  $\text{TE}_2$  mode was coupled out of the waveguide at a specific angle, spatially filtered, passed through interference filters, and detected by a photomultiplier tube. When the power density at the surface of the waveguide was less than  $5 \text{ MW cm}^{-2}$ , approximately 32 000 photons were generated with each pulse train. The CARS signal was normalized by dividing by the energy of the second harmonic of the beam at  $\omega_1$  produced in a KDP crystal and by the energy of the beam at  $\omega_2$ . The spectrum presented here was obtained by averaging 1000 pulse trains every  $0.2 \text{ cm}^{-1}$ . The resolution of the CARS spectrometer is  $1.6 \text{ cm}^{-1}$ .

The waveguide assembly was attached to a manipulator feedthrough with rotational and translational degrees of freedom. The manipulator was connected to the ultra-high-vacuum chamber through a flexible bellows. A 500-W tungsten filament was employed to irradiate the chamber walls. Another 100-W tungsten filament rested under the waveguide mount to heat the waveguide assembly. During a bake out the temperature of the waveguide was continuously monitored with a thermocouple which was connected to the rear surface of the waveguide. With prisms held in contact with the surface by an aluminum clamp, the waveguide surface could not be heated beyond  $100^\circ \text{C}$  without the risk of losing optical contact.

(18) Mazley, T.; Koenig, E. W.; Hetherington, W. M. *Chem. Phys.* **1987**, *116*, 113.

(19) Ho, Z. Z.; Wijekoon, W. M. K. P.; Koenig, E. W.; Hetherington, W. M. *J. Phys. Chem.* **1987**, *91*, 757.

(20) Hetherington, W. M.; Koenig, E. W.; Wijekoon, W. M. K. P. *Chem. Phys. Lett.* **1987**, *134*, 203.

(21) Wijekoon, W. M. K. P. Ph.D. Dissertation, University of Arizona, 1988.

(22) Fortenberry, R. M. Ph.D. Dissertation, University of Arizona, 1986.

(14) Stegeman, G. I.; Fortenberry, R. M.; Moshrefzadeh, R.; Hetherington, W. M.; Van Wyck, N. E.; Sipe, J. E. *Opt. Lett.* **1983**, *8*, 295.

(15) Hetherington, W. M.; Van Wyck, N. E.; Stegeman, G. I.; Fortenberry, R. M. *Opt. Lett.* **1984**, *9*, 88.

(16) Rabolt, J. F.; Santo, R.; Swalen, J. D. *Appl. Spectrosc.* **1980**, *34*, 517.

(17) Kogelnick, H. In *Integrated Optics*; T. Tamir, T., Ed.; Springer: Berlin, 1979.

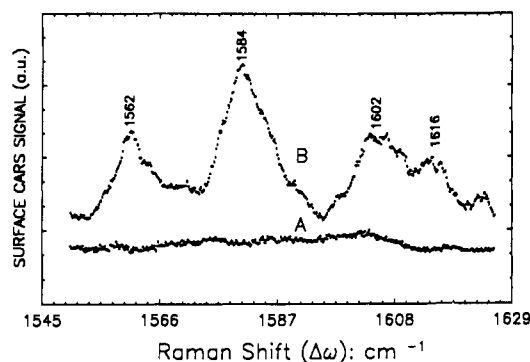


**Figure 1.** WSCARS spectra of (A) the bare ZnO surface at  $10^{-8}$  Torr and (B) after exposure to ethylene and evacuation to  $1 \times 10^{-3}$  Torr.

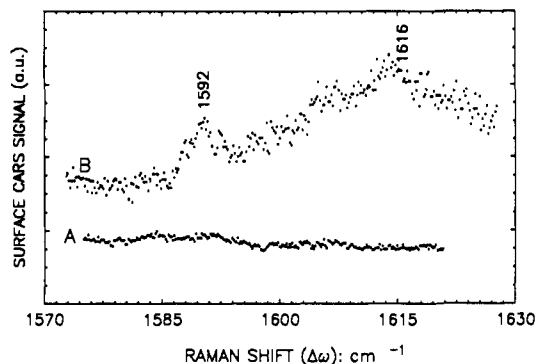


**Figure 2.** WSCARS spectra of (A) the bare ZnO surface at  $1 \times 10^{-6}$  Torr and (B) after exposure to ethylene and evacuation to  $2 \times 10^{-5}$  Torr.<sup>13</sup>

The ZnO surface was cleaned briefly by RF plasma etching before it was placed in the vacuum chamber. Once placed in the ultra-high-vacuum chamber, the waveguide as well as the entire chamber was baked at  $100^\circ\text{C}$  for 30 h. The base pressure of the chamber was  $2 \times 10^{-9}$  Torr. For adsorption experiments the chamber was filled with 5 Torr of ethylene and evacuated before a spectrum was taken. The samples were introduced into the chamber through a cold trap. The WSCARS spectra labeled as Figure 1A and 4A were taken at the chamber pressures  $1 \times 10^{-3}$  and  $5 \times 10^{-5}$  Torr, respectively. When the pressure of the system was about  $5 \times 10^{-5}$  Torr, 2 Torr of hydrogen was introduced into the chamber through a cold trap, and the spectrum shown in Figure 4B was recorded. The typical scan time for a spectrum was 45 min. For comparison a spontaneous Raman spectrum of ethylene dissolved in triply-distilled deionized water was obtained.

### Observations and Discussion

The WSCARS spectrum of a bare ZnO waveguide surface at  $1 \times 10^{-8}$  Torr is shown in Figure 1A. Upon exposure of the ZnO surface to 5 Torr of ethylene, followed by evacuation to  $1 \times 10^{-3}$  Torr, the WSCARS spectrum shown in Figure 1B is obtained. Both WSCARS spectra are drawn on the same vertical scale. Vacuum chamber evacuation to only  $1 \times 10^{-6}$  Torr, prior to introduction of ethylene, results in the appearance of the broad feature around  $1615\text{ cm}^{-1}$  shown in Figure 2B.<sup>13</sup> This indicates the presence of surface-confined hydroxyls since the WSCARS peaks corresponding to chemisorbed ethylene begin to appear only after evacuation of the sample chamber at  $1 \times 10^{-6}$  Torr for a period of 1 h. Furthermore, it was obvious from the time dependence of the WSCARS signal at  $1602\text{ cm}^{-1}$  when a bare ZnO waveguide surface which was evacuated to a pressure of  $1 \times 10^{-6}$  Torr was exposed to 1 Torr of ethylene. Approximately 25–30 mins were required (Figure 3) for complete adsorption, which may have been determined by diffusion of physisorbed ethylene onto a chemisorbed site.<sup>13</sup>

After the system was evacuated to  $5 \times 10^{-5}$  Torr, spectrum B in Figure 1 had evolved into that shown in Figure 4A. As the evacuation proceeds new features begin to appear with the disappearance of physisorbed ethylene. It was seen from a series

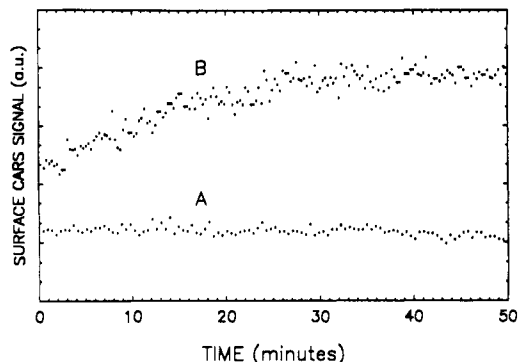


**Figure 3.** The time dependence of the WSCARS signal at  $1602\text{ cm}^{-1}$  with (A) 1 Torr of ethylene and (B) no ethylene present.<sup>13</sup>

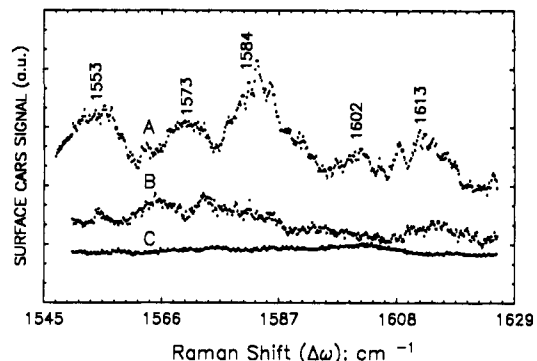


**Figure 4.** WSCARS spectra (A) 10 h after exposure to ethylene at  $5 \times 10^{-5}$  Torr and (b) after introduction of 2 Torr of hydrogen. The vertical scale of this spectrum is 0.6 times that of Figure 1. The background spectrum has been included in spectrum C.

of intermediate spectral scans that the relative intensity of the CARS peaks and their positions varied slightly from scan to scan. However, after 10 h of evacuation all the spectral features shown in Figure 4A had been well-resolved and could be reproduced very easily. The absolute and relative amplitudes of these WSCARS features varied slightly with the location of the interaction area of the laser fields on the waveguide surface and the extent of waveguide heating. All spectra reported here had no dependence upon the laser intensity at the surface.

In the previous study, evidence for the presence of at least four different types ( $\nu_{\text{C}=\text{C}}$  appearing at  $1615$ ,  $1602$ ,  $1590$ , and  $1580\text{ cm}^{-1}$ , respectively) of adsorbed ethylene on ZnO (0001) surface was presented.<sup>13</sup> However, at relatively higher surface coverages, observation of some of the adsorbed ethylene was difficult due to the presence of a thin hydroxyl coating on the surface. In this work all the previously observed surface species could be seen very easily. There is no quantitative estimate of the hydroxyl content on the waveguide surface; however, under the experimental conditions described above, surface hydroxyl density is largely reduced from its maximal coverage.<sup>23–26</sup>

All the spectral features shown in spectrum A of Figure 4 are attributed to chemisorbed ethylene due to the fact that they remain on the surface even after evacuation of the sample chamber for a period of 10 h, at  $5 \times 10^{-5}$  Torr. Clearly the diffusion of adsorbed ethylene among the chemisorption sites can be seen in Figure 4A. Initially there is very little CARS signal around  $1573$  and  $1553\text{ cm}^{-1}$  but within 2–3 h of evacuation distinct features begin to appear. As time progresses these peaks grow slowly and become

(23) Matmann, G.; Oswald, H. R.; Schweizer, F. *Helv. Chim. Acta* **1972**, *55*, 1294.

(24) Atherton, K.; Newbold, G.; Hockey, J. A. *Discuss. Faraday Soc.* **1971**, *52*, 33.

(25) Morimoto, T.; Nagao, M. *Bull. Chem. Soc.* **1972**, *43*, 3746.

(26) Nagao, M.; Morimoto, T. *J. Phys. Chem.* **1974**, *78*, 1116; **1980**, *84*, 2054.

(27) Hickernell, F. S. *Proc. IEEE* **1976**, *64*, 631.

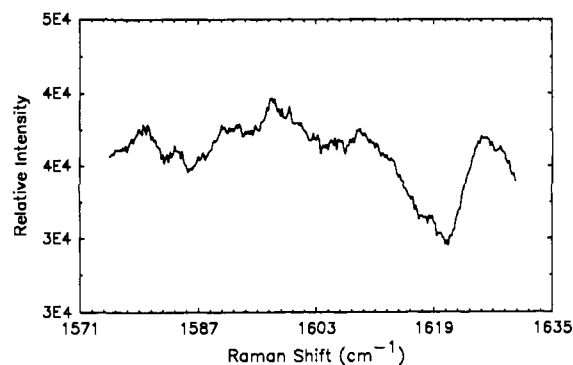


Figure 5. Spontaneous Raman spectrum of ethylene dissolved in triply-distilled deionized water after subtraction of the water spectrum.

well-established. The WSCARS peak around  $1553\text{ cm}^{-1}$  was not seen in the previous study since this spectral range was not examined. The peak positions of the two other previously reported species at  $1590$  and  $1580\text{ cm}^{-1}$  are found here to be  $1584$  and  $1573\text{ cm}^{-1}$ , respectively.

The Figure 4A indicates the presence of several different types of adsorbed ethylene on a ZnO(0001) surface. The observed long desorption times and the population times of some of these species could be consequences of the presence of residual hydroxyls on the surface. The WSCARS results were compared with a spontaneous Raman spectrum of ethylene dissolved in distilled, deionized water taken at the saturated concentration of about  $10^{-3}\text{ M}$  (Figure 5). After subtraction of the water spectrum, the only discernible features in this weak spectrum were a broad band at  $1626\text{ cm}^{-1}$  and a slight rise between  $1580$ ,  $1597$ , and  $1608\text{ cm}^{-1}$ . A surface density of ethylene corresponding to the saturated concentration in water would be too small to be observed in WSCARS spectra. A weak hydrogen bond ( $0.6\text{ kcal mol}^{-1}$ ) has been calculated to exist between ethylene and water.<sup>28</sup> Since only IR spectroscopy has been performed on such complexes in solid Ar at  $17\text{ K}$ , just  $\nu_2(\text{H}_2\text{O})$  of the  $\text{H}_2\text{O}\cdot\text{C}_2\text{H}_4$  complex has been seen at  $1595\text{ cm}^{-1}$ .<sup>29</sup> The observed  $\nu_2$  frequencies of water dimer and trimer are  $1611$ ,  $1593$ ,  $1632$ ,  $1620$ , and  $1602\text{ cm}^{-1}$ .<sup>30</sup> Therefore the reported WSCARS spectra are not that of surface bound water since no spectral features are apparent in the background spectrum (Figure 1A).

In the case of ZnO powders ethylene adsorption is rapid and reversible, and all the adsorbed ethylene can be recovered with a brief evacuation.<sup>4-6</sup> This indicates that the adsorbed ethylene, whatever its type, physisorbed or chemisorbed, is weakly held on the ZnO surface. However, our experimental observations do not seem to confirm these results. It is obvious due to lack of well-defined surface structure and homogeneity in powders that a variety of crystal planes are exposed to the adsorbate. On the basis of the surface atomic arrangements, the polarity largely varies from surface to surface.<sup>33</sup> The microstructure of the waveguide surface largely differs from that of ZnO single crystals and powders. The ZnO waveguide films are composed of densely packed crystallites oriented with all  $c$  axes perpendicular to the film. The crystallite size is approximately  $80\text{ nm}$ .<sup>27</sup> This (0001) waveguide surface is dominated by the coordinatively unsaturated zinc ions, and therefore, we assign all the WSCARS features that appear in Figure 4A to  $\nu_{\text{C}=\text{C}}$  vibrations of ethylene adsorbed on  $\text{Zn}^{2+}$  sites which are in different chemical environments. Further, the  $\nu_{\text{C}=\text{C}}$  frequencies for ethylene  $\pi$ -bonded to a variety

of metal ions and metals lie in the spectral range between  $1470$  and  $1585\text{ cm}^{-1}$ .<sup>34-36</sup>

Correlation of observed  $\nu_{\text{C}=\text{C}}$  frequencies with the heats of adsorption measured by Yasuda for ethylene adsorbed on ZnO powders brings up the question of the use of empirical relationship between  $\Delta\nu$  and  $\Delta H$ . Self-consistent-field ab initio calculations result in interaction energy of  $-1.07\text{ kcal mol}^{-1}$  for ethylene  $\pi$ -bonded to the  $\text{Zn}^{2+}$  ion.<sup>31</sup> The calculation has assumed a  $\pi$ -complex of  $C_{2v}$  symmetry for the reaction intermediate. This calculated energy correlates well with the observed  $\nu_{\text{C}=\text{C}}$  around  $1600\text{ cm}^{-1}$ . However, the existence of several adspecies of different bond energies cannot be explained with such calculations. On the other hand, other computations<sup>32</sup> show that even for complexes of ethylene of moderate strength, the experimentally observed value,  $\Delta\nu_{\text{C}=\text{C}} = \nu_{\text{C}=\text{C}}^{\text{gas}} - \nu_{\text{C}=\text{C}}^{\text{bond}}$  cannot serve as a quantitative measure of the variations of the C=C bond strength only. Rather, peak positions reflect the change in the electron density on and between the C-H bonds. Therefore, the observed  $\nu_{\text{C}=\text{C}}$  frequencies may indicate the perturbation of the ethylene adsorbed on  $\text{Zn}^{2+}$  sites by the neighboring residual surface hydroxyls and nearby adsorbates.

After 2 Torr of hydrogen was introduced into the sample chamber, most of the WSCARS signal disappears, indicating that the hydrogenation of adsorbed ethylene takes place (Figure 4B). It was found that the shape of this spectrum (Figure 4B) is approximately the same even if the introduction of the hydrogen was made at  $1 \times 10^{-3}$  Torr. It is interesting to notice the amplitude of the CARS signal around  $1602\text{ cm}^{-1}$ . This  $\pi$ -complex underwent hydrogenation on ZnO powders as probed by IR spectroscopy.<sup>4-6</sup> As seen in the spectrum the amplitude of the CARS signal around  $1602\text{ cm}^{-1}$  coincides with the background signal level, indicating that the adspecies is completely removed from the surface. Also, this species desorbs more easily than the rest of the species (compare signal levels in Figures 1B and 4A). Both of these observations are in accord with the previously reported results by Dent and Kokes.<sup>4-6</sup> However, the relative surface density of this species (Figure 4A) is smaller than that of other surface species. Both low and higher energy branches of the spectrum have relatively larger WSCARS amplitude, indicating that the relative surface density of the corresponding species is larger.

The relatively higher amplitude of the CARS signal on both the higher and the lower energy sides of the  $1602\text{-cm}^{-1}$  band in spectrum B in Figure 4 compared to the background indicates the presence of trace amounts of residual ethylene on the surface. These relative amplitude levels are not affected by evacuation of the sample chamber for a period of 10 h at  $5 \times 10^{-6}$  Torr or by introduction of a new hydrogen dose. However, after 10 h of heating the waveguide at  $50\text{ }^\circ\text{C}$  with occasional introduction of oxygen into the chamber, approximately the same background spectrum shown in Figure 1A can be generated. The basic sequence of spectra presented in Figures 1 and 4 can be reproduced with respect to the spectral features and approximate time dependence of the features.

We recognize several other possibilities which can give rise to the observed higher WSCARS amplitude after introduction of hydrogen. First, if the hydrogenation of ethylene took place resulting in carbonaceous species (as in the case of pure metals<sup>1</sup>), these products may contaminate the waveguide surface, and the resulting surface can be different from that of the cleaned surface. Therefore, the amplitude of the signal can be different from that of the initial ZnO surface. Second, if we assume that all the adsorbed ethylene is hydrogenated, the excess hydrogen can be dissociatively adsorbed on ZnO, leading to the formation of a partially hydroxylated surface which is different from the original ZnO surface.<sup>22-25</sup> In fact, hydrogenation of ethylene has been

(28) Del Bene, J. E. *Chem. Phys. Lett.* **1974**, *24*, 203.

(29) Engdahl, A.; Nelander, B. *Chem. Phys. Lett.* **1985**, *113*, 49.

(30) Banes, A. J.; Suzuki, S. *J. Mol. Struct.* **1981**, *70*, 301.

(31) Gropen, O.; Haaland, A.; Defrees, D. *Acta Chem. Scand.* **1985**, *A39*, 367.

(32) Burgina, E. B.; Yurchenko, E. N. *J. Mol. Struct.* **1984**, *116*, 17.

(33) Akhter, S.; Lui, K.; Kung, H. H. *J. Phys. Chem.* **1985**, *89*, 1958.

(34) Little, L. H. *Infrared Spectra of Adsorbed Species*; Academic Press: New York, 1966.

(35) Patterson, M. L.; Weaver, M. J. *J. Phys. Chem.* **1985**, *89*, 1331.

(36) Diella, P. *Chem. Phys. Lett.* **1980**, *73*, 500.

shown to occur at surface sites which are capable of dissociative adsorption of hydrogen. We disregard the first possibility since we were able to generate approximately the same spectrum shown in Figure 1A after heating the waveguide. If carbon residues are present on the surface, cleaning the surface can be very tedious. Also, in our earlier work<sup>13</sup> we found that some of the adsorbed ethylene on ZnO (0001) cannot be removed without heating the surface. Furthermore, formation of carbonaceous species during the hydrogenation of ethylene on ZnO is not known. We rule out the second possibility on the basis of the following observations. If the surface hydroxyls are responsible for the residual higher amplitude levels, at least some of the hydroxyl should be removed with evacuation, and the signal levels should be affected. We do not see any remarkable change in the amplitude levels even after prolonged evacuation (10 h) or after introduction of a new dose of hydrogen. Furthermore, the WSCARS spectrum of a ZnO surface which was exposed to hydrogen at  $5 \times 10^{-5}$  Torr does not show any significant features in this spectral region. Thus, the higher residual WSCARS amplitude cannot be attributed to surface hydroxyls or adsorbed hydrogen. Therefore, the conclusion can be reached that there are trace amounts of adsorbed ethylene on the surface which do not undergo hydrogenation. The residual ethylene may have

attached to the catalytically inactive sites on the surface. Although the ZnO (0001) surface is dominated by  $Zn^{2+}$  ions, surface defects (pin holes, kink etc.) may expose other surface sites for ethylene adsorption which are not catalytically active.

### Conclusion

Incorporation of integrated optical techniques with surface vibrational spectroscopy has provided a sensitive means to study adsorption-desorption phenomena and catalytic reaction of adsorbates on well-defined crystalline surfaces. It is possible to study the rates of desorption and population and the rate of hydrogenation of different types of surface-bound ethylene using WSCARS. Also, by performing WSCARS of transient species (surface ethyl in the present case) one can learn more about the surface dynamics and reaction pathways of catalytic reactions. Furthermore, WSCARS can be used to measure the dephasing time ( $T_2$ ) of monolayer coverage of adsorbates.

**Acknowledgment.** We thank W. R. Salzman, G. I. Stegeman, R. M. Fortenberry, and T. Bradshaw for many helpful discussions. The help provided by J. Pemberton in Raman measurements of ethylene adsorbed in water is also acknowledged. This work was supported by the National Science Foundation.